The Phosphorylation of Vinculin on Tyrosine Residues 100 and 1065, Mediated by Src Kinases, Affects Cell Spreading

Zhiyong Zhang,* Gonzalo Izaguirre,* Siang-Yo Lin,* Hwa Young Lee,* Erik Schaefer,[†] and Beatrice Haimovich*[‡]

*Department of Surgery and the Cancer Institute of New Jersey, Robert Wood Johnson Medical School-University of Medicine and Dentistry of New Jersey, New Brunswick, NJ 08903; and [†]BioSource International, Hopkinton, MA 01748

Vinculin is a conserved actin binding protein localized in focal adhesions and cell-cell junctions. Here, we report that vinculin is tyrosine phosphorylated in platelets spread on fibrinogen and that the phosphorylation is Src kinases dependent. The phosphorylation of vinculin on tyrosine was reconstituted in vanadate treated COS-7 cells coexpressing c-Src. The tyrosine phosphorylation sites in vinculin were mapped to residues 100 and 1065. A phosphorylation-specific antibody directed against tyrosine residue 1065 reacted with phosphorylated platelet vinculin but failed to react with vinculin from unstimulated platelet lysates. Tyrosine residue 1065 located in the vinculin tail domain was phosphorylated by c-Src in vitro. When phosphorylated, the vinculin tail exhibited significantly less binding to the vinculin head domain than the unphosphorylated tail. In contrast, the phosphorylation did not affect the binding of vinculin to actin in vitro. A double vinculin mutant protein Y100F/Y1065F localized to focal adhesion plaques. Wild-type vinculin and single tyrosine phosphorylation mutant proteins Y100F and Y1065F were significantly more effective at rescuing the spreading defect of vinculin null cells than the double mutant Y100F/Y1065F. The phosphorylation of vinculin by Src kinases may be one mechanism by which these kinases regulate actin filament assembly and cell spreading.

INTRODUCTION

Cell spreading is a complex process requiring a bidirectional transmembrane linkage between the extracellular matrix and the actin cytoskeleton. Most cell-substrate interactions are mediated by members of the integrin superfamily of transmembrane adhesion receptors (Hynes, 2002). Integrin-activating ligands trigger changes in receptor conformation and receptor clustering, which in turn activate signaling events leading to the assembly of focal complexes and actin filament networks (Critchley, 2000; Emsley et al., 2000; Liu et al., 2000; Geiger et al., 2001; Kim et al., 2003; Ridley et al., 2003). Vinculin is one of the first actin binding proteins recruited into focal complexes and subsequently focal adhesion plaques (Geiger et al., 1980; Zaidel-Bar et al., 2003). Vinculin is composed of a large 95-kDa globular head and a 30-kDa tail linked by a short proline-rich sequence (Coutu and Craig, 1988). The three regions serve as docking sites for several proteins. Actin and paxillin bind to sequences located in the vinculin tail domain (Menkel et al., 1994; Wood et al., 1994; Huttelmaier et al., 1997; Goldmann et al., 1998). Talin and α-actinin bind to the vinculin head domain, whereas members of the Ena/VASP and ponsin/ArgBP52/ vinexin families, as well as the Arp 2/3 complex, interact with the proline-rich region in vinculin (Kawabe et al., 1999; Mandai et al., 1999; Critchley, 2000; DeMali et al., 2002).

Biochemical and structural studies established that vinculin exists in at least two distinct conformations dependent upon an intramolecular interaction between its head and tail domains (Johnson and Craig, 1994; Winkler et al., 1996; Bakolitsa et al., 1999, 2004; Borgon et al., 2004; Izard et al., 2004). Binding of the head to the tail domain results in a "closed conformation" that limits accessibility of vinculin-binding proteins to their docking sites. It is currently thought that acidic phospholipids, which bind to the vinculin tail domain, transiently disrupt head–tail interactions and enable the binding of ligands such as talin, VASP, and protein kinase C (PKCα), to their respective sites (Gilmore and Burridge, 1996; Weekes et al., 1996; Huttelmaier et al., 1998; Steimle et al., 1999; Ziegler et al., 2002; Bakolitsa et al., 2004). PKCα phosphorylates vinculin on at least two serine residues in positions 1033 and 1045; the role of the phosphorylation is currently not fully understood (Ziegler et al., 2002). Izard et al. (2004) recently reported that binding of talin derived peptides to vinculin triggered marked conformational changes in vinculin and head-tail displacement. These observations raised the possibility that various inputs might either activate specific repertories of vinculin-dependent signaling events or determine the duration of downstream signals.

Vinculin null embryos did not survive past embryonic day 10, demonstrating that vinculin plays a key role during embryonic development (Xu et al., 1998a). The role of vinculin relative to cell spreading, however, is currently not fully understood. Vinculin null fibroblasts assembled focal

adhesion plaques, and yet, spread poorly on fibronectin (Xu *et al.*, 1998b), suggesting that vinculin might regulate the dynamics of actin filament assembly. The interaction between vinculin and Arp 2/3 uncovered by DeMali and Burridge (DeMali *et al.*, 2002) provided insight into one mechanism by which vinculin may execute its regulatory function. More recently Subauste *et al.* (2004) reported that vinculin modulates the interaction between paxillin and focal adhesion kinase (FAK), which in turn affected extracellular signal-regulated kinase signaling required for cell survival and motility. These findings revealed a previously unappreciated layer of interactions involving vinculin.

Vinculin was one of the first identified tyrosine phosphorylation substrates of v-Src, the transforming oncogene of Rouse sarcoma virus (Sefton *et al.*, 1981). The v-Src–dependent phosphorylation sites in vinculin were not mapped (Ito *et al.*, 1983). Tyrosine phosphorylation of vinculin was observed in platelets stimulated by Ca^{2+} (Vostal and Shulman, 1993) and more recently in leukotriene D(4)-treated intestinal epithelial cells (Massoumi and Sjolander, 2001). In an effort to characterize a protein of 120 kDa that is heavily tyrosine phosphorylated in spread platelets, we identified the protein as vinculin. We also found that the phosphorylation of vinculin in platelets is regulated by Src kinases. The phosphorylation of vinculin was reconstituted in COS-7 cells cotransfected with c-Src and the tyrosine phosphorylation sites were mapped to residues 1065 and 100. A vinculin double mutant protein, Y100F/Y1065F, was less effective than wild-type vinculin in rescuing the spreading defect of vinculin null cells on fibronectin. These findings suggest that the phosphorylation of vinculin by Src kinases might affect early events in cell spreading.

MATERIALS AND METHODS

Antibodies and Cell Lines

Monoclonal antibodies (mAbs) 4G10 and PY-20 were purchased from Upstate Biotechnology (Lake Placid, NY) and BD Transduction Laboratories (San Diego, CA). The mAbs to human vinculin (hVin-1 and V9131) or to chicken vinculin (VIN-115) were from Sigma-Aldrich (St. Louis, MO). The mAb against 6-His was purchased from QIAGEN (Valencia, CA). The vinculin-null mouse embryo fibroblasts (Vin −/−) (Xu *et al.*, 1998a) were a gift from E. Adamson (Burnham Institute, La Jolla, CA). The Vin −/− clone used in this study was identical to the clone used by DeMali and Burridge (DeMali *et al.*, 2002). The COS-7 and the NIH 3T3 cells were from the American Tissue Type Culture Collection (Manassas, VA).

Platelet Isolation

Human platelets were isolated by gel filtration as described previously (Haimovich *et al.*, 1993). Platelets were lysed immediately or were adhered for 1 h to fibrinogen (100 µg/ml; Sigma-Aldrich) coated onto the surface of electrically untreated polystyrene plates as described previously (Haimovich *et al.*, 1993). Where indicated, platelets were treated for 30 min with 5 µM PP2 (Calbiochem, San Diego, CA) before exposure to the fibrinogen-coated plates. Unstimulated and adherent platelets were lysed with 2% SDS in buffer containing 66 mM Tris, pH 7.4, 1 mM vanadate, and 1 mM phenylmethylsulfonyl fluoride (PMSF).

Isolation and Characterization of a ~120-kDa Platelet Phosphoprotein

Platelets were purified by gel-filtration from 5 U of outdated platelets (purchased from the New Jersey Blood Bank, New Brunswick, NJ). To activate the platelets and to induce aggregation, the platelet suspension was stirred vigorously for 20 min with 10 nM of phorbol 12-myristate 13-acetate (PMA). The resulting platelet aggregates were collected by 5-min centrifugation at 800 × *g*. The platelet pellet was resuspended in 6 ml of lysis buffer containing 50 mM Tris-HCl, pH 8.0, 0.02% Triton X-100, 1 mM EGTA, 1 mM Na_3VO_4, and 1 mM PMSF. The cell suspension was sonicated briefly to disrupt the aggregates. All subsequent steps were carried out at 4°C. The lysate was cleared by 20-min centrifugation at 17,000 × *g*, and the resulting supernatant was loaded onto a Sephacryl-300 HR column (1.6 × 70 cm). Fractions were collected at a constant flow of 0.32 ml/min. Proteins were resolved by SDS-PAGE and transferred to a nitrocellulose membrane. The pattern of tyrosine phosphorylated proteins

in each fraction was analyzed by immunoblotting and probing with monoclonal antibody (mAb) 4G10. Fractions 6–11 were combined and dialysis-concentrated against 50 mM Tris buffer, pH 8.0, containing 1 mM vanadate. The pooled fraction (4 ml) was loaded onto a DEAE-Sepharose column (1.2 × 14 cm) preequilibrated with 50 mM Tris buffer, pH 8.0, containing 1 mM vanadate. The column was washed with 30 ml of loading buffer, and proteins were eluted off the column with 40 ml of 50 mM Tris buffer, pH 8.0, containing a linear gradient of NaCl concentration from 0 to 0.5 M and 1 mM vanadate. Fractions containing the 120-kDa protein were identified as described above. Fractions 3–5 (total volume 4.5 ml) were pooled, concentrated (final concentration ~1 mg/ml), and analyzed by two-dimensional (2-D) gel electrophoresis and Coomassie Blue staining. The gel segment containing the 120-kDa protein was cut out from the Coomassie Blue-stained gel and sent to the W.M. Keck Foundation Biotechnology Resource Laboratory (Yale University, New Haven, CT) for analysis and identification by matrix-assisted laser desorption ionization/mass spectrometry (MALDI-MS). The mass of 18 peptides obtained from a tryptic digest of the sample matched the predicted mass of vinculin-derived peptides.

Western Blotting Analysis

Proteins resolved by SDS-PAGE were blotted onto either a polyvinylidene diflouride (PVDF) or a nitrocellulose membrane. The membranes were probed sequentially with mAb 4G10 and the mAb to human- or chicken-vinculin. Secondary antibody was horseradish peroxidase-conjugated rabbit anti-mouse (Bio-Rad, Hercules, CA). Immunoreactive bands were visualized by chemiluminescence using enhanced chemiluminescence reagents (PerkinElmer Life and Analytical Sciences, Boston, MA).

2-D Gel Electrophoresis

Suspended or fibrinogen-adherent platelets were lysed in boiling buffer containing 2% SDS and 66 mM Tris, pH 8.0. Isoelectric focusing of samples containing 100 µg of protein per sample was carried out by Kendrick Labs (Madison, WI) as described previously (Izaguirre et al., 1999).

Immunoprecipitation of Phosphorylated Vinculin from Platelets

Fibrinogen adherent platelets were lysed in radioimmunoprecipitation assay buffer (1% Triton X-100, 1% deoxycholic acid, 10 mM Tris-HCl, pH 7.2, 158 mM NaCl, 0.1% SDS, 1 mM Na_3VO_4, and 1 mM PMSF). The lysates were precleared for 1 h with 40 µl of protein A/G agarose beads followed by an overnight incubation with mAb PY-20. Antibody–antigen complexes were precipitated with 50 µl of protein A/G agarose beads, eluted with sample buffer, and analyzed by SDS-PAGE.

Proteolytic Digestion of Platelet Vinculin

Activated platelet lysates were resolved by SDS-PAGE on a 7.5% T acrylamide gel (18 cm in length, 1.5 mm in thickness). One-half of the gel was blotted onto nitrocellulose. To verify the phosphorylation of vinculin and its position on the gel, the membrane was probed sequentially with the mAbs to vinculin and to phosphotyrosine. The second half of the gel was stained with Coomassie Blue R-250 for 2 h and destained overnight. The gel was rehydrated in water until it regained its original dimension. The area of the gel containing vinculin was excised and placed in a microcentrifuge tube. Each gel piece was washed for 5 min with 300 µl of 50% acetonitrile and then for 30 min each with the same volumes of 50% acetonitrile, 50 mM NH_4HCO_3, pH 8.0, followed by 50% acetonitrile, 10 mM NH_4HCO_3, pH 8.0. After the last wash, the gel pieces were dried by lyophilization and stored below 4°C. In gel proteolytic digestions of vinculin were carried out with carboxylpeptidase Y (0.22 µg/µl; Sigma-Aldrich) in 50 mM citrate buffer, pH 6.0. The dehydrated gel pieces were first rehydrated on ice for 30 min with 20 µl of buffer plus enzyme (twofold concentrated). The volume was increased to 40 µl by adding buffer, and the samples were incubated at 37°C for the indicated time. The digestion was terminated by the addition of 50 µl of Laemmli's loading buffer (4×) and by heating for 2 min at 100°C. The samples (including the gel pieces) were loaded onto a SDS-PAGE gel. Proteins resolved on the gel were transferred to nitrocellulose and analyzed by Western blotting and immunodetection.

Molecular Cloning and Mutagenesis

The complete cDNA encoding for chicken vinculin (Coutu and Craig, 1988) kindly provided by Susan W. Craig (John Hopkins University, Baltimore, MD) was subcloned in frame into the *Eco*RI site of a pQE-31 vector (QIAGEN), resulting in the addition of a 6-His tag to the carboxy-terminal end of vinculin. The gene was then subcloned into the *Eco*RI site of pcDNA3.1(+) (Invitrogen, San Diego, CA) for mammalian expression. The tyrosine residues at positions 100, 160, 537, 822, and 1065 were replaced by phenylalanines by single base substitution (TAT to TTT) by using QuikChange site-directed mutagenesis (Stratagene, La Jolla, CA). The Y100F/Y1065F double mutant was generated by two cycles of mutagenesis. The introduction of the expected mutations was confirmed by DNA sequencing. The same approach was used to introduce the

Y100F, Y1065F, and Y100F/Y1065F substitutions in vinculin cloned into the pEGFP vector (kindly provided by Susan W. Craig). To introduce glutamic acid substitutions in place of the tyrosine residues at position 100 and 1065, the TAT in the appropriate positions were changed to GAG by site-directed mutagenesis. The double mutant Y100E/Y1065E was generated using two cycles of mutagenesis.

Expression of Recombinant Proteins in COS-7 Cells

Cells were transfected using the Lipofectamine Plus reagents (Invitrogen) following the protocol recommended by the vendor. Briefly, cells cultured in 10-cm dishes were cotransfected with 3 μg of wild-type or mutant vinculin cDNAs and 1 μg of a constitutively active c-Src cDNA (Y529F) (kindly provided by David Schlaepfer, Scripps Research Institute, La Jolla, CA). Vanadate (1 mM) prepared as described previously (Izaguirre *et al.*, 2001) was added to the cell culture medium 48 h after transfection. The cells were cultured in the presence of vanadate for 24 h before analysis. Proteins were immunoprecipitated as described previously (Izaguirre *et al.*, 2001).

Generation of Antibodies Specific for the Phosphorylated Y1065 Residue in Vinculin

A rabbit polyclonal antibody against the phosphorylated tyrosine residue 1065 (anti-vinculin [pY1065]) was generated by BioSource International (Hopkinton, MA) by using the peptide VRKTPW[pY]Q. To verify the antibody specificity, COS-7 cells were transfected with recombinant wild-type and mutant vinculin cDNAs as described above, and lysates containing 500 μg/ml protein were subjected to immunoprecipitation with an antibody to the His tag. The immunoprecipitated proteins were resolved by SDS-PAGE and were Western blotted with the anti-vinculin[pY1065] antibody at a final concentration of 0.2 μg/ml. For Western blotting of total platelet lysates, the antibodies were first preabsorbed against unstimulated platelet lysates resolved by SDS-PAGE and then subjected to Western blotting as indicated above. Antibody specificity was also verified by peptide competition for which the anti-vinculin [pY1065] antibody (6 μg) was first incubated for 1 h at room temperature with the phosphopeptide immunogen (60 μg) (BioSource International) in a final volume of 70 μl. The treated antibody was then used in Western blotting of platelet lysates.

In Vitro Src Kinase Assay

The expression plasmids encoding the His-tagged chicken vinculin head (V1-851) and tail (V884-1066) domains were described previously (Johnson and Craig, 2000) and were kindly provided by Susan W. Craig. Fusion proteins were produced in *Escherichia coli* BL21(DE3) cells treated with isopropyl β-D-thiogalactoside (IPTG) and purified as described previously (Johnson and Craig, 2000). His tagged-vinculin tail or head domains (1 μg each) were incubated with 7.5 U/sample of constitutively active c-Src kinase (Upstate Biotechnology) in the presence of 10 μCi of [γ-^{33}P]ATP in 25 μl of phosphorylation buffer (20 mM MOPS, pH 7.4, 5 mM MnCl$_2$, 5 mM MgCl$_2$, 1 mM dithiothreitol [DTT], 0.5 mM sodium vanadate). Phosphorylation was carried out for 15 min at 37°C. Reactions were terminated by the addition of Laemmli's sample buffer and heating for 5 min at 100°C. Proteins were resolved by SDS-PAGE and transferred to a PVDF membrane. Incorporation of [γ-^{33}P]ATP was visualized by autoradiography. To immunodetect the recombinant vinculin tail and head domains, respectively, membranes were probed with the mAbs to His and to vinculin.

Expression and Purification of Glutathione S-Transferase Fusion Proteins

The plasmid encoding the glutathione *S*-transferase (GST)-tagged chicken vinculin head domain (GST/V1-855) (Johnson and Craig, 1994) was a generous gift from Susan W. Craig. The GST-tagged protein was expressed and purified as described previously (Johnson and Craig, 1994).

Vinculin's Head–Tail Interaction

Purified His-vinculin-tail (His-Tail) (0.75 μg/sample) was incubated in the presence or absence of c-Src, and the in vitro kinase assay was carried out as described above. After the kinase reaction, the total volume of the sample was adjusted to 450 μl with TEEAN buffer containing 0.5% CHAPS, 0.1 mM Na$_3$VO$_4$, and 1 mM PMSF. The Ni^{2+}-NTA agarose beads were collected by a brief centrifugation and washed twice to remove the c-Src kinase. The resulting phosphorylated and unphosphorylated His-tail proteins immobilized on Ni^{2+}-NTA agarose beads were incubated for 3 h at 25°C with purified GST/V1-head at the indicated concentration. Incubations (400 μl) were performed in TEEAN buffer supplemented with 0.5 mM β-mercaptoethanol and 1% bovine serum albumin. The samples were collected by brief centrifugation and washed four times in TEEAN. To elute the bound proteins, the Ni^{2+}-NTA agarose pellets were heated in electrophoresis sample buffer. Eluted proteins were subjected to SDS-PAGE. Phosphorylation of the vinculin tail domain was analyzed by autoradiography and immunoblotting.

Vinculin-Actin Cosedimentation Assay

To obtain unphosphorylated- and phosphorylated-vinculin, respectively, COS-7 cells were cotransfected with cDNAs encoding for wild-type vinculin and c-Src and were either untreated or treated with vanadate as described above. The His-tagged recombinant proteins in the phosphorylated and unphosphorylated form were purified on Ni^{2+}-agarose columns as described previously (Izaguirre *et al.*, 2001). Actin (1.6 μM; Cytoskeleton, Denver, CO) and vinculin (0.05 μM) were incubated for 2 h at room temperature in a final volume of 250 μl containing 1.5 mM Tris, pH 8.0, 0.04 mM CaCl$_2$, 0.1 mM DTT, 100 mM KCl, 2 mM MgCl$_2$, 1 mM ATP, 1 mM PMSF, and 0.1 mM Na$_3$VO$_4$. An aliquot (50 μl) representing the total protein content was removed from each sample before the sedimentation. The samples (200 μl each) were sedimented for 30 min at 95,000 $\times$ g (Steimle *et al.*, 1999) in a Discovery M150 SE Micro ultraspeed centrifuge (Sorvall, Newton, CT) by using the S120AT3 rotor. The supernatants were separated from the pellets, and the pellets were resuspended in 50 μl of SDS-PAGE sample buffer. Samples (35 μl each) representing a fraction of the initial reaction mix and the supernatant, and the entire pellet, were resolved by SDS-PAGE and Western blotting with the indicated antibodies.

Vinculin Null Cells Spreading Assay

The vinculin-null mouse embryo fibroblasts (Vin $-/-$) were maintained in DMEM supplemented with 10% fetal bovine serum and cultured in 5% CO$_2$ at 37°C. Control cells were only transfected with a vector encoding for a puromycin-resistant gene (pPUR; BD Biosciences Clontech, Palo Alto, CA). All other groups were cotransfected with the pPUR vector plus green fluorescent protein (GFP) tagged-vinculin constructs at a ratio of 4:1. The cells were treated with puromycin at a concentration of 2 μg/ml starting at 24 h posttransfection. The puromycin-resistant cultures (we did not select clones) were propagated and expanded for ~2 wk. To determine the level of expression of the recombinant proteins, lysates containing 20 μg of protein was subjected to Western probing with the mAb to human vinculin.

To determine the effect of reconstituted vinculin on cell spreading, puromycin-resistant cell populations were trypsinized and replated onto fibronectin (10 μg/ml) (Calbiochem) coated surfaces for 2 h. The cultures were fixed for 20 min with 3.7% formaldehyde, washed three times with phosphate-buffered saline (PBS), and examined by light microscopy by using a Nikon Eclipse TE200 microscope equipped with a 20$\times$/0.45 objective. For each cell population, a total of at least 500 cells distributed in six randomly selected fields were scored as either spread or round. Experiments were repeated three times. Data represent the average $\pm$ S.D. The data were analyzed using an unpaired t test. The statistical analysis was performed using the StatView software from Abacus Concepts (Berkeley, CA).

Immunolocalization

NIH 3T3 cells were transfected with the GFP-tagged vinculin constructs by using the Lipofectamine Plus reagents. The cells were trypsinized at 24 h posttransfection and were replated for 24 h onto fibronectin (20 μg/ml) precoated glass coverslips. The cells were fixed, permeabilized for 10 min with 0.1% Triton-X-100 in PBS, and stained with Texas red-phalloidin (1:100; Molecular Probes, Eugene, OR) in PBS containing 1% bovine serum albumin. The cells were visualized using an LSM 510 confocal microscope (Carl Zeiss, Thornwood, NY) equipped with a 60$\times$/1.4 water objective.

RESULTS

Vinculin Is Tyrosine Phosphorylated in Spread and/or Aggregated Platelets

Numerous proteins are tyrosine phosphorylated in activated platelets. Stable phosphorylation of several of these proteins, including phosphoproteins of 101 and 120 kDa, as well as α-actinin (105 kDa) (Figure 1A, lane 2), are only detected when platelets are fully spread on fibrinogen or when they are stimulated with PMA to form large aggregates. Our initial goal was to identify and characterize the phosphoprotein of 120 kDa (pp120), which we partially purified from PMA-stimulated outdated platelets (Izaguirre *et al.*, 1999). The activated platelets were lysed in buffer containing 0.02% Triton X-100, and soluble proteins were fractionated by sequential chromatography on a Sephacryl 300-HR and a DEAE-Sepharose column. Western blotting and probing with mAb 4G10 identified fractions containing pp120 (Figure 1, B and C). Fractions eluted off the DEAE-column that contained pp120 were combined and analyzed by Coomassie Blue staining (Figure 1D). The section of the gel containing pp120 was excised and analyzed by MALDI-MS. The
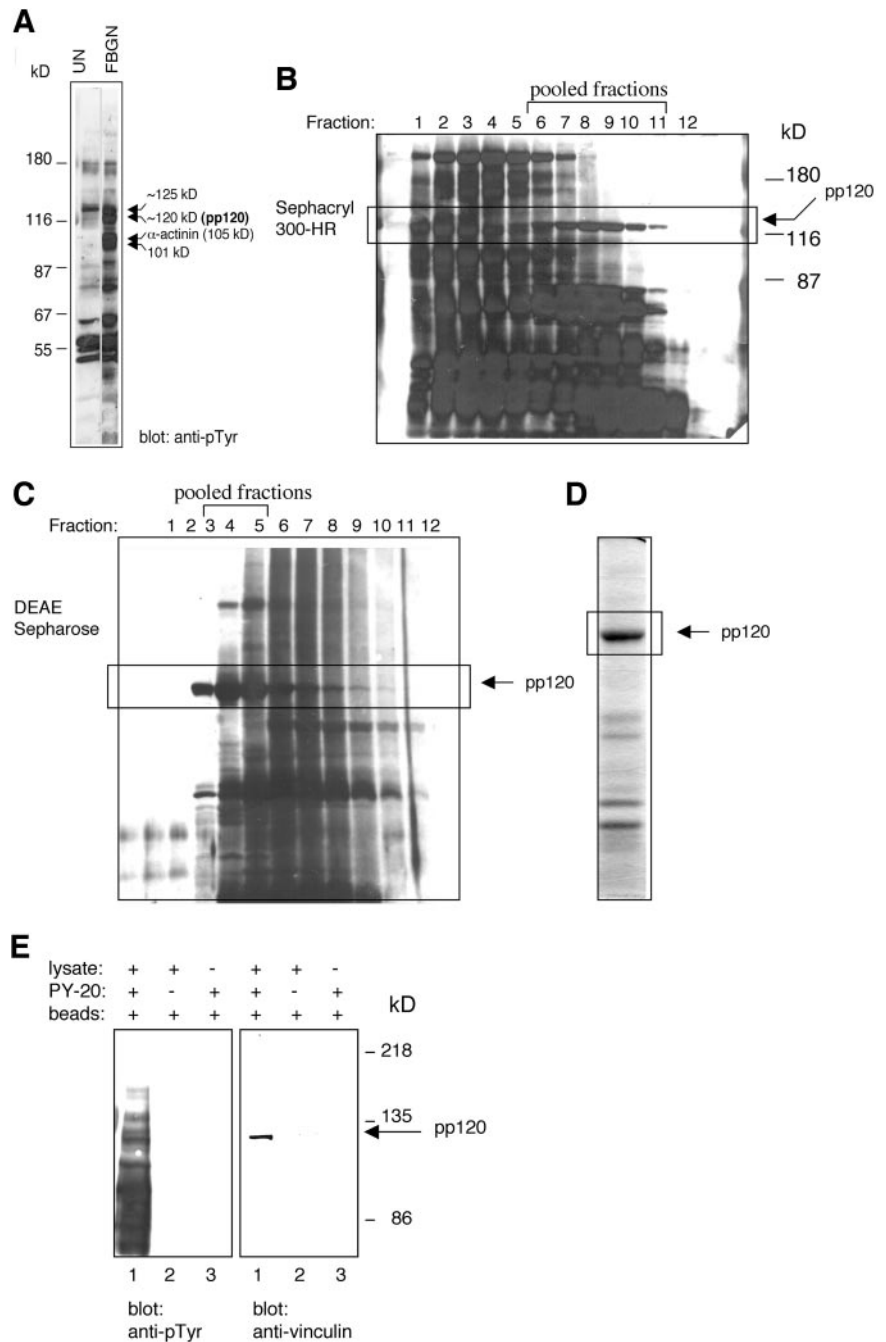
Figure 1. Partial purification of a 120-kDa tyrosine phosphorylated protein from activated platelets. (A) Gel-filtered platelets were unstimulated (UN) or were adhered and spread on fibrinogen for 1 h (FBGN), and lysates were probed on Western blots with mAb 4G10. Arrowheads mark the position of the tyrosine phosphorylated proteins of 101 kDa, 105 kDa/α-actinin, 120 kDa (pp120), and 125 kDa. The location of the molecular weight standards is indicated on the left. PMA-activated platelet lysates were used as the source material for the purification of pp120. Soluble proteins were fractionated by gel filtration on a Sephacryl 300-HR (B) and a DEAE-Sepharose (C) column. The pattern of tyrosine phosphorylated proteins in each fraction was determined by Western blotting with mAb 4G10. Details are described in *Materials and Methods*. (D) A final fraction containing pp120 was analyzed by SDS-PAGE and Coomassie Blue staining. The 120-kDa protein band was identified by MALDI-MS as vinculin. (E) Activated platelet lysates were immunoprecipitated with mAb PY-20 (lane 1). Control samples included a lysate incubated without the primary antibody (lane 2) or with the primary antibody alone (lane 3). Immunoprecipitates were subjected to Western blot analysis with mAb 4G10 (anti-pTyr) and the mAb to vinculin.

mass of 18 peptides obtained from a tryptic digest of the sample matched the predicted mass of human vinculin-derived peptides (unpublished data), indicating that pp120 is platelet vinculin.

Because phosphorylated vinculin was not immunoprecipitated using commercially available mAbs to vinculin (unpublished data), we took a reversed approach and immunoprecipitated vinculin with a generic mAb to phosphotyrosine, PY-20. As shown in Figure 1E, a protein of 120 kDa immunoprecipitated by mAb PY-20 was recognized by the mAb to vinculin by Western blotting.

To further confirm that vinculin is tyrosine phosphorylated in activated platelets, lysates of unstimulated platelets (Figure 2A) and fibrinogen-adherent platelets (Figure 2B)

were analyzed by two-dimension gels and Western blotting. The samples were resolved on parallel gels and transferred to PVDF membranes. The membranes were stained with Coomassie Blue to visualize the general pattern of resolved proteins, destained, and probed with mAb 4G10 and the mAb to human vinculin. The region of the membrane containing vinculin is marked by a rectangle. Platelet activation did not significantly alter the migration profile of most proteins detected by staining of the membranes with Coomassie Blue (Figure 2). Vinculin migrated between pI 6.6 and 7.6. The broad migration pattern of vinculin reflects the multiple vinculin isoforms (five) identified in platelets (Bruin *et al.*, 1991; Gravel *et al.*, 1995). Platelet spreading on fibrinogen did not significantly alter the electrophoretic mobility of
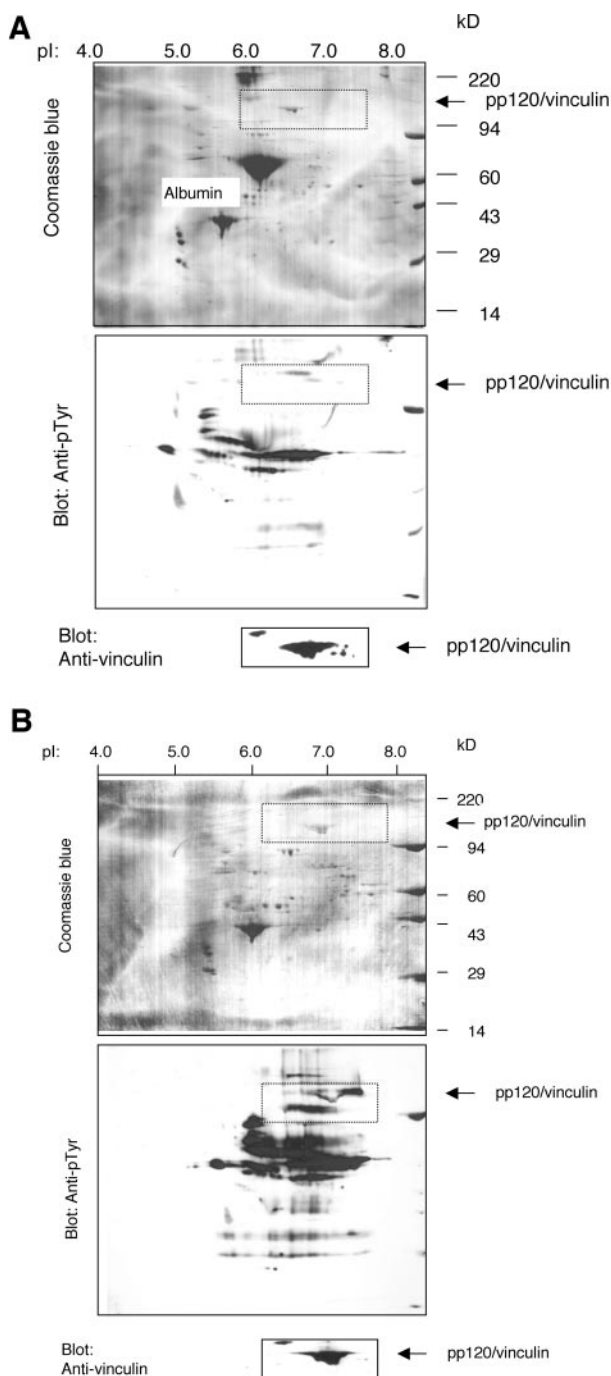
Figure 2. Two-dimension analysis reveals colocalization of pp120 and vinculin. Platelets were unstimulated (A) or spread on a fibrinogen-coated surface (B) for 1 h. Lysates containing 100 µg of protein were resolved on parallel gels and transferred onto PVDF membranes. The membranes were stained with Coomassie Blue, destained, and probed sequentially with mAb 4G10 and the mAb to human vinculin. The position of albumin derived from the buffer in which the isolated platelets were lysed is indicated in A. The rectangles mark parallel areas of the membranes. (C) Vinculin and the tyrosine phosphorylated proteins migrating with, or adjacent to, vinculin shown within the areas marked by rectangles in B were traced, and the traces were superimposed as shown. The data demonstrate that vinculin and pp120 colocalize.

vinculin. As expected, and previously shown (Izaguirre *et al.*, 1999), platelet activation resulted in a significant increase in the number and intensity of tyrosine phosphorylated proteins. The region of the membrane containing vinculin in the unstimulated platelets revealed only trace reactivity with mAb 4G10 (Figure 2A). In contrast, two tyrosine-phosphorylated proteins were noted in the same region of the membrane containing the fibrinogen-adherent platelet lysate (Figure 2B). One tyrosine phosphorylated protein colocalized to the lower region of vinculin. A second tyrosine phosphorylated protein migrated immediately above and at the basic end of vinculin (Figure 2, B and C). These findings established that vinculin is the only protein of 120 kDa

detected by this method of analysis exhibiting robust tyrosine phosphorylation in spread platelets.

Treatment of Platelets with an Inhibitor of Src Kinases, PP2, Prevents Spreading and Tyrosine Phosphorylation of Vinculin

Vinculin was one of the first proteins found to be phosphorylated on tyrosine by the transforming gene product of Rous sarcoma virus, pp60[src] (v-Src) (Sefton *et al.*, 1981; Ito *et al.*, 1983). Platelets express a high concentration of pp60[c-src] (c-Src), the cellular homologue of v-Src (Golden *et al.*, 1986) as well as several other Src kinase family members (Huang *et al.*, 1991). To examine whether Src kinases regulate the
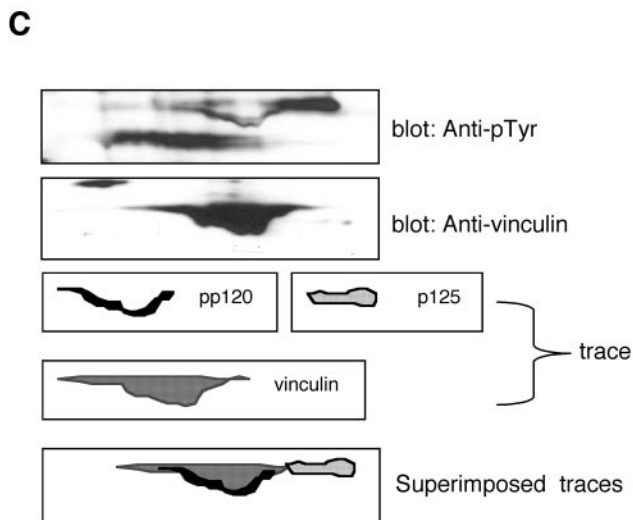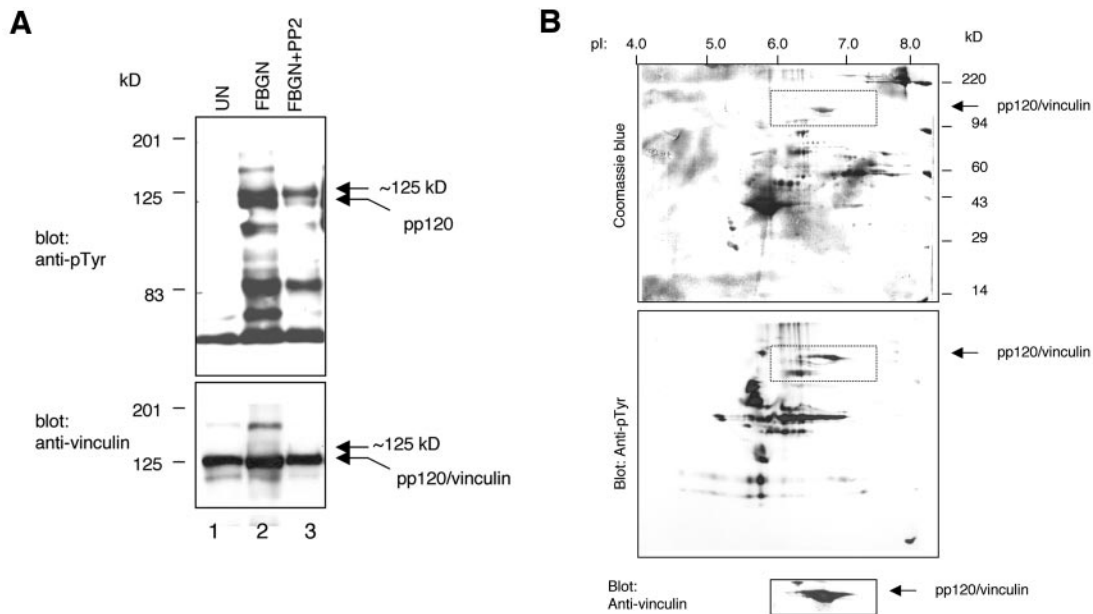
Figure 3. Phosphorylation of vinculin on tyrosine is affected by the inhibitor of Src kinases, PP2. (A) Platelets were unstimulated (UN), adhered, and spread on fibrinogen for 1 h (FBGN), or treated with 5 μM PP2 for 1 h before adherence to fibrinogen (FBGN + PP2). Samples containing equal protein amounts (15 μg) were probed on Western blots with mAb 4G10 and the mAb to vinculin. (B) Platelets treated with PP2, as described above, were lysed and analyzed on a two-dimension gel. The rectangles mark parallel areas of the membranes. The data shown demonstrate that PP2 greatly reduced the phosphorylation of vinculin on tyrosine. PP2 did not affect the phosphorylation of the 125-kDa protein.

phosphorylation of vinculin in platelets, platelets were treated with the inhibitor of Src kinases PP2 (Hanke *et al.*, 1996) before adhesion to a fibrinogen-coated surface. Consistent with the results reported by Obergfell *et al.* (2002), we also found that PP2 inhibited platelet spreading on fibrinogen (unpublished data). Lysates of untreated platelets and PP2-pretreated platelets were analyzed by Western blotting. As shown in Figure 3A, the phosphorylation of vinculin was significantly reduced by PP2. In contrast, the phosphorylation of the 125-kDa tyrosine phosphorylated protein migrating immediately above vinculin was only minimally affected by the inhibitor. These findings were confirmed by analysis of the PP2-pretreated platelet sample by 2-D gels. To enable accurate comparison between the PP2-treated and the untreated samples, the gel shown in Figure 3B and those shown in Figure 2 were run in parallel and were processed at the same time. PP2 eliminated the reactivity of mAb 4G10 with pp120/vinculin but had no effect on the antibody reactivity with the 125-kDa protein (Figure 3B). These results established that pp120/vinculin and pp125 are two distinct proteins. These findings also provided a strong indication that the phosphorylation of vinculin on tyrosine in platelets is Src kinases dependent.

Vinculin Is Tyrosine Phosphorylated on Residues 100 and 1065

Because platelets are not amenable to genetic manipulations, we sought to establish a model cell system in which the phosphorylation of vinculin could be further investigated. As COS-7 cells are more resistant to vanadate than other cell types (e.g., NIH 3T3 cells), we constructed and expressed a recombinant His-tagged vinculin (His-vinculin) cDNA in these cells. His-vinculin was successfully expressed in COS-7 cells, but the protein was not phosphorylated either in the absence or the presence of vanadate (Figure 4). However, coexpression of

His-vinculin with a constitutively active form of c-Src (Y529F) resulted in robust phosphorylation of vinculin. The phosphorylation of vinculin was only detected in cells treated with vanadate, indicating that in the absence of vanadate vinculin is rapidly dephosphorylated by an endogenous phosphatase. Endogenous vinculin immunoprecipitated with the mAb to vinculin also was phosphorylated in vanadate-treated cells cotransfected with c-Src (Figure 4C). The phosphorylation of the endogenous vinculin was somewhat variable, and in some experiments (Figure 5), it was barely detectable. Based on these findings, the phosphorylation of vinculin was examined in all subsequent experiments in COS-7 cells that were cotransfected with c-Src and treated with vanadate.

Vinculin contains 8 tyrosine residues (Figure 5A). Protease V8 cleaves vinculin in the proline-rich region (amino acid residues 837–879) to produce two major vinculin fragments: a 95-kDa head domain and a 30-kDa tail domain (Johnson and Craig, 1994). Seven of the eight tyrosine residues found in vinculin are located in the head domain. The only tyrosine residue located in the vinculin tail domain is positioned at residue 1065, one amino acid residue away from its carboxy-terminal end (Figure 5A). To begin to map the phosphorylation site(s) in vinculin, fibrinogen-adherent platelet lysates were resolved by SDS-PAGE, and the region of the gel containing phosphorylated vinculin was excised and subjected to in-gel digestion with carboxypeptidase Y, a proteolytic enzyme that removes amino acids from the carboxy-terminal end. Carboxypeptidase Y eliminated the reactivity of mAb 4G10 with the phosphorylated vinculin within minutes (unpublished data). These data provided the first indication that vinculin is phosphorylated on tyrosine residue 1065 in platelets.

To further investigate the phosphorylation sites in vinculin, the tyrosine in position 1065 was changed to phenylalanine by site-directed mutagenesis (Figure 5). The mutant
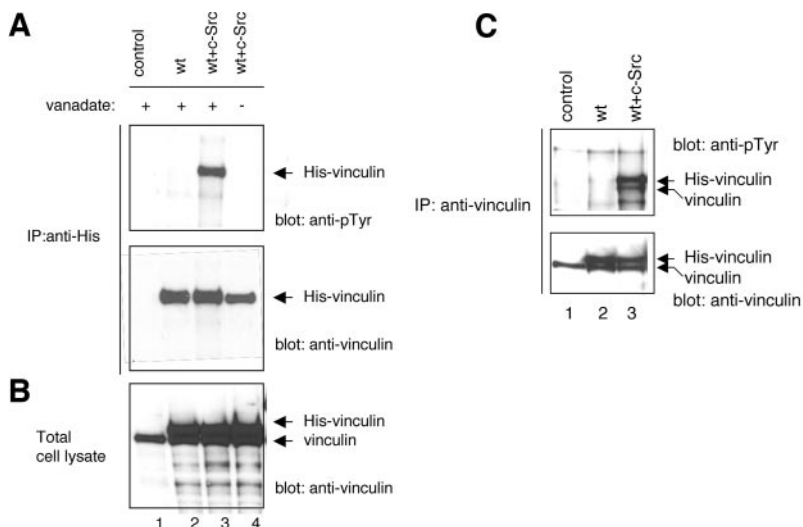
Figure 4. Vinculin is tyrosine phosphorylated in vanadate treated COS-7 cells coexpressing c-Src. COS-7 cells were untransfected (control, lane 1), transfected with wild-type His-vinculin alone (wt; lane 2), or cotransfected with wild-type His- vinculin and a constitutively active *c-src* (Y529F) cDNA (wt + c-Src; lanes 3 and 4). At 48 h posttransfection, the cells were either untreated (lane 4) or treated for 24 h with vanadate (lanes 1–3). (A) Lysates containing equal protein amounts were subjected to immunoprecipitation with a mAb to His, and the immunoprecipitates were probed on Western blots as indicated. (B) Lysates containing equal protein amounts (15 μg/sample) were analyzed by Western blotting with a mAb to vinculin. (C) COS-7 cells transfected and treated as described above were subjected to immunoprecipitation with a mAb to vinculin. The immunoprecipitates were probed by Western blotting as indicated.

protein Y1065F immunoprecipitated from COS-7 cells by using the mAb to His exhibited significantly less phosphorylation than the wild-type protein, suggesting that residue 1065 is a phosphorylation site (Figure 5B). However, Western blotting of the proteins immunoprecipitation by using the mAb to vinculin, revealed no difference in the level of phosphorylation between the recombinant wild-type vinculin and the Y1065F mutant (Figure 5D). The simplest interpretation of these data was that vinculin is phosphorylated

on more than one site. We speculate that the mAb to vinculin has a low affinity or does not recognize the population phosphorylated on residue 1065. This could explain why the mAb to vinculin failed to immunoprecipitate phosphorylated vinculin from activated platelets. To identify a second phosphorylation site in vinculin five additional tyrosine residues were individually changed to phenylalanines by site directed mutagenesis. The tyrosine residues chosen for site directed mutagenesis included residue 822 implicated as a
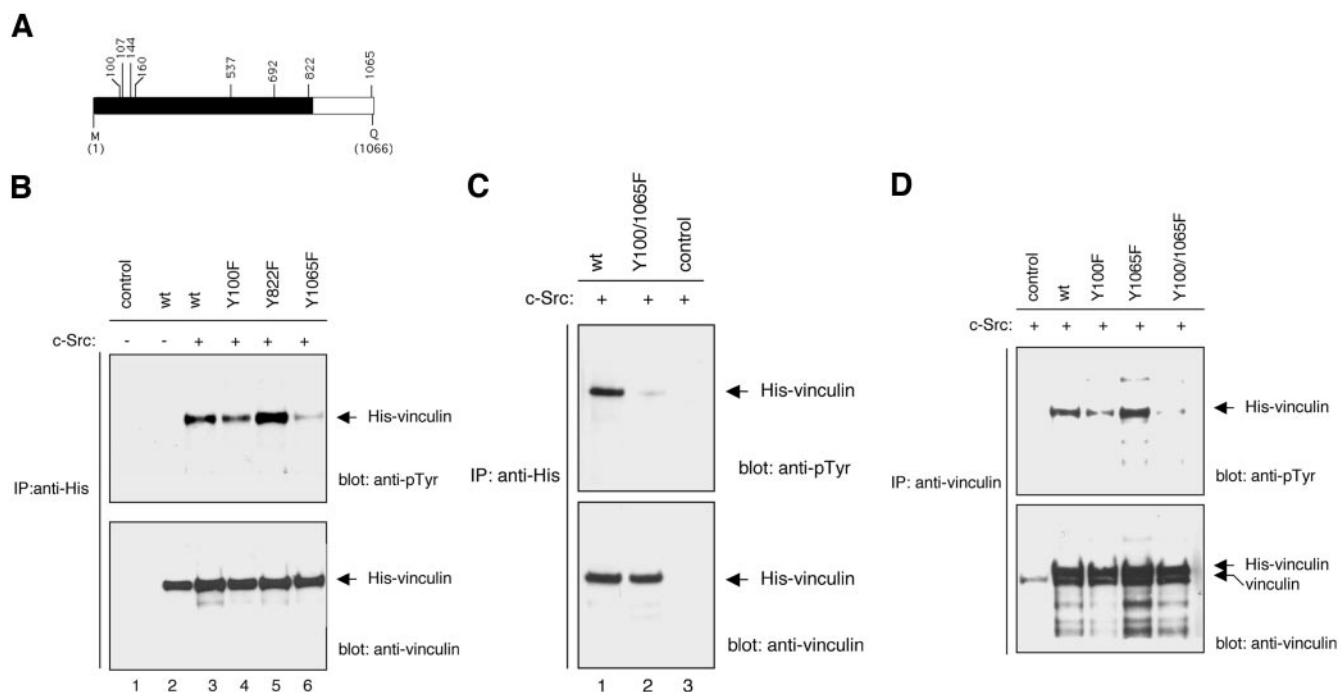

Figure 5. Vinculin is tyrosine phosphorylated on residues 100 and 1065. (A) Schematic diagram of the eight tyrosine residues found in vinculin. The black-and-white areas represent, respectively, the vinculin head and tail domains. (B–D) COS-7 cells were not transfected (control) or were transfected with cDNAs encoding for wild-type His-vinculin (wt), the His-vinculin point mutants Y100F, Y822F, and Y1065F, or the His-vinculin double mutant Y100F/Y1065F. The cells were transfected with the His-vinculin construct alone (B, lane 2) or were cotransfected with a cDNA encoding for a constitutively active c-Src. The cultures were treated with vanadate for 24 h before lysis. Lysates containing equal protein amounts were immunoprecipitated with the mAb to His (B and C) or the mAb (D) to vinculin. The immunoprecipitates were probed with the indicated antibodies.

phosphorylation site by other investigators (Goldmann and Ingber, 2002), and residues 100, 160, 537, and 692. Pinna and Ruzzene (1996) proposed that Src kinase family members require a hydrophobic residue at n-1 for optimal phosphorylation. Because a charged residue precedes the tyrosine residues in positions 107 and 144, these residues were not included in the first round of mutagenesis. The mutant proteins were coexpressed with c-Src in COS-7 cells. As shown in Figure 5, B and D, the Y100F mutant exhibited less phosphorylation than wild-type vinculin. In contrast, the phosphorylation of Y822F (Figure 5), Y160F, Y537F, or Y692F mutants (unpublished data) did not significantly differ from that of wild-type vinculin. Building on these data, we next generated a Y100F/Y1065F double mutant. The Y100F/Y1065F double mutant protein immunoprecipiated by the mAbs to either His or vinculin was not phosphorylated (Figure 5, C and D), indicating that tyrosine residues 100 and 1065 are the primary, if not the only, tyrosine phosphorylation sites in vinculin.

To confirm that platelet vinculin is phosphorylated on tyrosine residue 1065, a phosphorylation site-specific rabbit polyclonal antibody was generated against tyrosine residue 1065. To verify the antibody specificity, recombinant wild-type and mutant His-vinculin proteins expressed in COS-7 cells were immunoprecipitated with an antibody to His and were analyzed by Western blotting and probing with the anti-vinculin [pY1065] antibody. The antibody reacted with phosphorylated wild-type vinculin and the Y100F mutant protein but failed to react with either the Y1065F or Y100F/Y1065F mutant proteins (Figure 6A). These data established that the anti-vinculin [pY1065] antibody is phosphotyrosine 1065 site specific. Unstimulated and fibrinogen adherent platelet lysates were next subjected to Western blotting analysis with the same antibody. As shown in Figure 6B, the antiserum reacted with vinculin extracted from platelets adherent to fibrinogen but did not react with vinculin extracted from unstimulated platelets. Furthermore, the antibody reactivity was completely blocked by the phosphopeptide immunogen. These findings established that platelet vinculin is phosphorylated on tyrosine residue 1065. It remains to be determined whether platelet vinculin is phosphorylated on tyrosine residue 100 and/or any other site.

c-Src Phosphorylates Vinculin on Residue 1065 In Vitro

To examine whether tyrosine residues 100 or 1065 are bona fide c-Src substrates, His-tagged vinculin tail (V884-1066) and head (V1-851) domain proteins expressed in *E. coli* were purified on Ni^{2+}-agarose columns and subjected to in vitro kinase assays in the presence of recombinant c-Src. The vinculin tail domain, but not the vinculin head domain, was phosphorylated by c-Src in vitro (Figure 7). These findings established that c-Src can phosphorylate vinculin on residue 1065, which is the only tyrosine residue in the tail domain. The mechanism by which vinculin is phosphorylated on residue 100 remains presently unclear. We also have found that intact vinculin was not phosphorylated by c-Src in vitro, raising the possibility that the tail residue is inaccessible to the kinase (unpublished data).

The Phosphorylation of Vinculin on Tyrosine Residue 1065 Affects Head–Tail Interaction

Biochemical studies were the first to suggest that the vinculin head and tail domains are involved in intramolecular interactions (Johnson and Craig, 1994). To examine whether the phosphorylation of vinculin on its tail domain affected head–tail interactions, GST-tagged head (GST-head) and His-tagged tail (His-tail) domain proteins were expressed
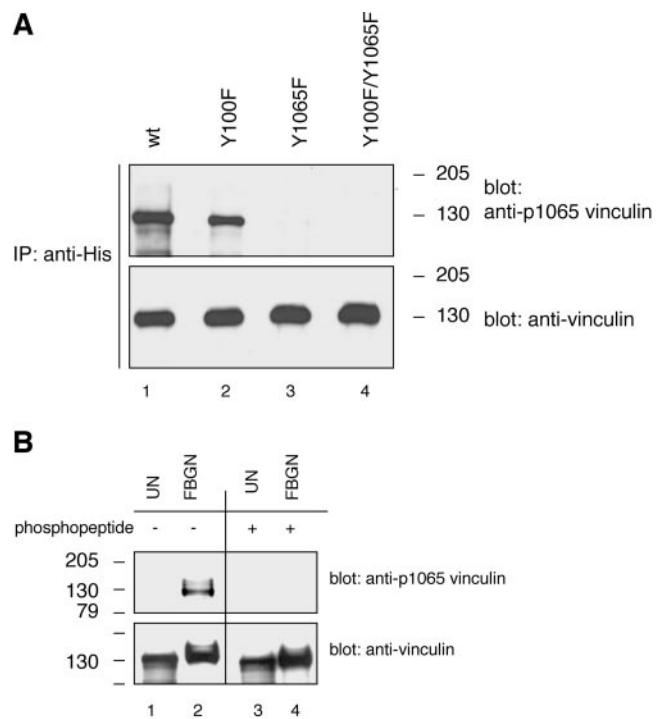
Figure 6. Phosphorylation site-specific antibody recognizing vinculin when phosphorylated on tyrosine residue 1065 reacts with platelet vinculin. (A) COS-7 cells were cotransfected with a constitutively active c-Src (Y529F) cDNA and with cDNAs encoding for wild-type His-vinculin (wt; lane 1), the His-vinculin point mutants Y100F (lane 2) and Y1065F (lane 3), or the His-vinculin double mutant Y100F/Y1065F (lane 4). The cells were treated and lysed as described in the legend to Figure 3. Lysates containing equal protein amounts were subjected to immunoprecipitation with a mAb to His, and the immunoprecipitates were analyzed by Western blotting and probing with a rabbit polyclonal antiserum raised against a phosphopeptide immunogen mimicking the phosphorylated tyrosine residue 1065 in vinculin (anti-vinculin[pY1065]). The blot was stripped and reprobed with the antibody to vinculin. (B) Unstimulated (UN) and fibrinogen (FBGN)-adherent platelet lysates (15 μg/sample) were probed by Western blotting with the anti-vinculin[pY1065] antiserum that was not treated (lanes 1 and 2) or that was blocked with the phosphopeptide immunogen (lanes 3 and 4). The blot was stripped and reprobed with the antibody to vinculin.

and purified from IPTG-induced BL21 *E. coli*. The His-tail was immobilized on Ni^{2+}-NTA beads. Uncoated- and His-tail-coated beads were subsequently incubated with GST-head. As shown in Figure 8, A and B, the GST-head did not bind to the beads in the absence of His-tail. In the presence of His-tail, however, the GST-head was pulled-down in a concentration-dependent manner, reaching a plateau at a 1:1 ratio of His-tail to GST-head. These data indicated that this assay could quantify head–tail interactions when the His-tail is used in excess relative to the GST-head.

In the next set of experiments, the His-tail was either not phosphorylated or was phosphorylated by c-Src in vitro. Unphosphorylated or phosphoryated His-tail proteins immobilized on Ni^{2+}-NTA agarose beads were incubated with GST-head at a ratio of 3:1 (0.75 μg of His-tail: 0.25 μg of GST-head). As shown in Figure 8B, although the GST-head was effectively pulled down by the unphosphorylated His-tail, the GST-head was not pulled down by the phosphorylated His-tail. These data indicated that the phosphorylation of vinculin on residue 1065 affects head–tail interaction.
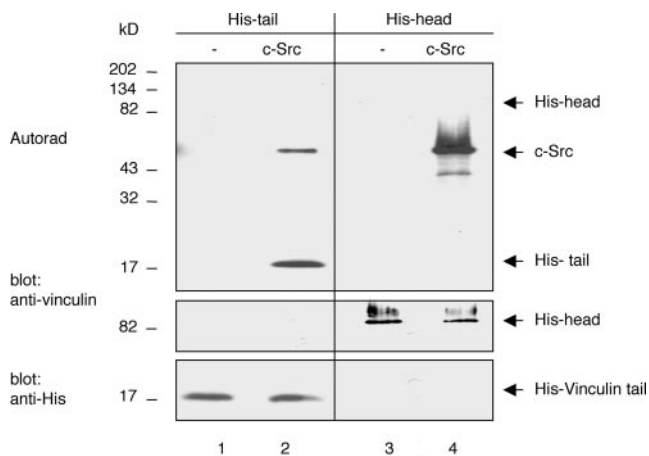
Figure 7. Vinculin tail domain is phosphorylated in vitro by c-Src. Purified, recombinant His-vinculin tail (His-tail) and -head (His-head) domain proteins were incubated for 15 min in kinase buffer containing 10 μCi of [γ-^{33}P]ATP without (lanes 1 and 3) or with c-Src (7.5 U/reaction) (lanes 2 and 4). Reaction products were resolved by SDS-PAGE and transferred to a PVDF membrane. Incorporation of [γ-^{33}P]ATP was detected by autoradiography (Autorad). The membrane was subsequently probed with the mAb to vinculin and to His to confirm, respectively, equal loading of the head and tail domain proteins.

The Phosphorylation of Vinculin on Tyrosine Residues 100 and 1065 Does Not Affect the Interaction between Vinculin and Actin In Vitro

An intramolecular association between the vinculin head and tail domains masks the actin binding site in vinculin (Johnson and Craig, 1995) and prevents the cosedimentation of intact vinculin with actin filaments. We considered the possibility that the phosphorylation of vinculin on tyrosine residues 100 and 1065 may alter the actin binding properties of intact vinculin. To test for this possibility recombinant vinculin in either their phosphorylated and unphosphorylated form were purified and subjected to cosedimentation with polymerized actin. The data shown in Figure 9 demonstrate that as previously shown for unphosphorylated vinculin, phosphorylated vinculin also failed to cosediment with actin filaments suggesting that the phosphorylation of vinculin by Src did not trigger a conformational change that was sufficient to expose the actin-binding site in vinculin.

Vinculin Phosphorylation Mutants Localize to Focal Adhesion Plaques

To examine whether the phosphorylation of vinculin affects its cellular localization, we used GFP-tagged wild-type vinculin as a template to generate Y100F, Y1065F, and Y100F/Y1065F mutant constructs. The proteins were expressed in NIH 3T3 cells. The GFP-tagged wild-type and mutant vinculin proteins localized to focal adhesion plaques, indicating that the cellular localization of vinculin is not affected by its state of phosphorylation on tyrosine (Figure 10). Further studies are required to determine whether the phosphorylation affects cell migration and/or the rate of assembly or turnover of focal adhesion plaques.

The Phosphorylation of Vinculin on Tyrosine Residues 100 and 1065 Affects Cell Spreading

To determine whether the phosphorylation of vinculin on tyrosine residues 100 and/or 1065 affects cell spreading,
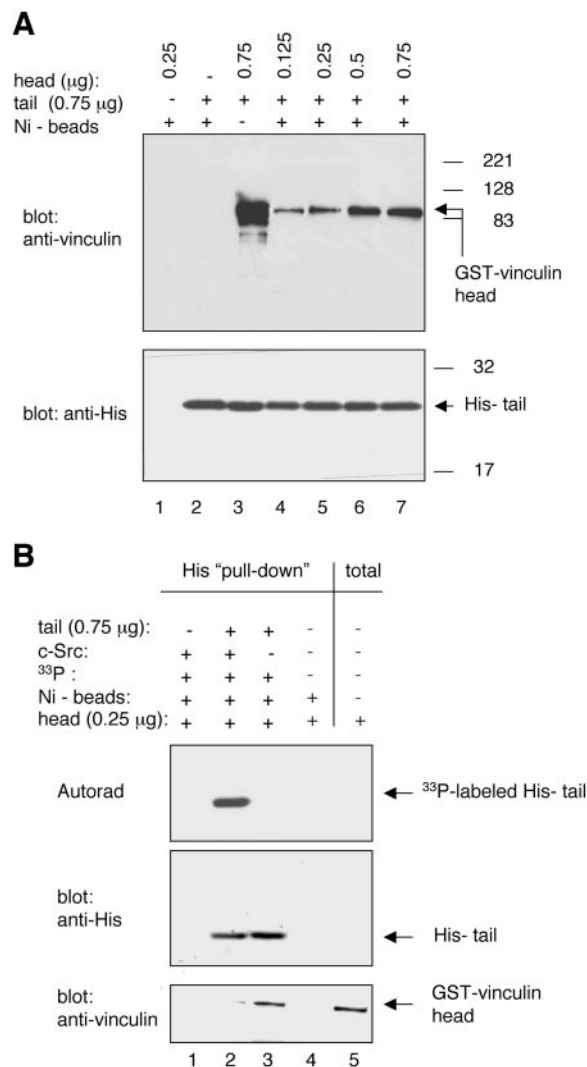

Figure 8. Phosphorylation of tyrosine residue 1065 affects vinculin head-tail interactions. (A) GST-tagged vinculin head domain protein (V1–855) at the indicated concentration was incubated for 3 h at 25°C with the His-tagged vinculin tail domain protein (V884-1066; 0.75 μg/sample). Complexes were pulled down with Ni^{2+}-NTA agarose beads and were analyzed by Western blotting with the indicated antibodies. (B) His-tail domain protein (V884-1066; 0.75 μg/sample) was either not phosphorylated or was phosphorylated by c-Src in vitro by using the kinase assay described above. The tail proteins were immobilized onto Ni^{2+}-NTA agarose beads as described in *Materials and Methods*. The tail–bead complexes were incubated for 3 h at 25°C with the GST-head domain protein (V1-855; 0.065 μg/sample). Bound proteins were eluted off the beads and analyzed by autoradiography (Autorad) and by Western blotting with the indicated antibodies. Results are representative of three experiments.

GFP-tagged wild-type and vinculin mutant proteins were expressed in vinculin null cells (Vin −/−) (Xu *et al.*, 1998b). Effort to identify vinculin reconstituted cells based on the fluorescence of the GFP tag was unsuccessful due to the fact that the fluorescence signal was very weak. To circumvent this problem, the vinculin null cells were cotransfected with GFP-vinculin constructs and a vector encoding for a puromycin resistant gene (Gu *et al.*, 1999). A control group was transfected with only the puromycin-encoding vector. Puromycin-resistant populations were propagated and expanded
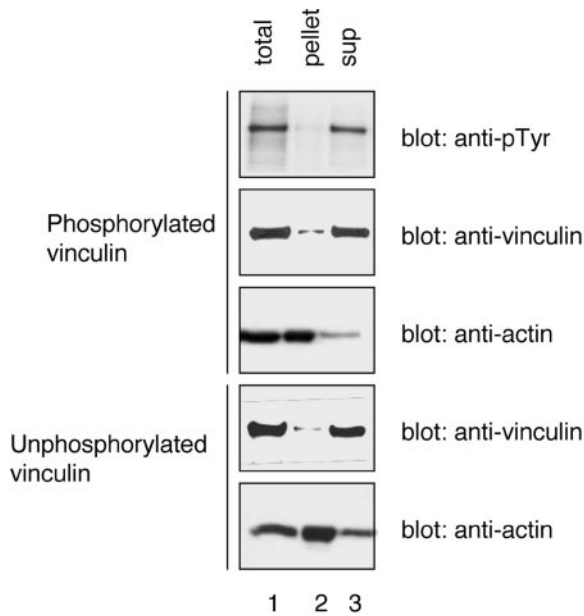
Figure 9. Phosphorylation of vinculin on tyrosine residue 100 and 1065 does not affect its binding to actin. Recombinant phosphorylated and unphosphorylated vinculin were purified from transfected COS-7 cells. The purified proteins (0.05 μM) were incubated for 2 h with actin (1.6 μM) in polymerization buffer. An aliquot was removed from each sample before the sedimentation (lane 1; total). The samples then were subject to centrifugation at $100,000 \times g$ for 30 min. The supernatants were removed and the pellets were resuspended in sample buffer. Equal volumes from each sample were analyzed by SDS-PAGE and Western blotting with the indicated antibodies.

for 2 wk. The cultures transfected with the various vinculin constructs plus puromycin expressed equal levels of wild-type and mutant vinculin proteins as determined by a West-

ern blotting analysis of equal protein amounts (Figure 11A). To compare the spreading ability of vinculin null cells to cells expressing wild-type vinculin or vinculin mutant proteins, the puromycin resistant cell populations were plated on fibronectin-coated surfaces for 2 h, fixed, and examined by light microscopy. As previously reported and shown in Figure 11, B and C, few (13 $\pm$ 2%) of the control cells expressing only the puromycin-resistant gene were spread, whereas 60 $\pm$ 7% of the cells expressing wild-type vinculin were spread on fibronectin within 2 h. The number of spread cells expressing Y100F or Y1065F mutant proteins was statistically indistinguishable from that of cells expressing wild-type vinculin (56 $\pm$ 65 and 53 $\pm$ 64%, respectively). In contrast, 36 $\pm$ 5% of the cells expressing the Y100F/Y1065F double mutant protein were spread, representing a ~40% decrease in the number of spread cells relative to the three other cell populations. The difference between the cells expressing the double mutant protein and the cells expressing wild-type vinculin, or the mutant proteins Y100F and Y1065F, was statistically significant (p $\leq$ 0.001) for all three comparisons.

We reasoned that if the phosphorylation of vinculin on tyrosine residues 100 and 1065 positively regulates cell spreading, then the introduction of negatively charged amino acid residues in the same positions may enhance cell spreading. To test this hypothesis, single and a double tyrosine to glutamic acid substitutions were introduced to generate Y100E, Y1065E, and Y100E/Y1065E mutants. The proteins were expressed in the vinculin null cells as described above. The expression of the recombinant proteins was verified by Western blotting (unpublished data). We observed no statistically significant difference in spreading among the cells expressing wild-type vinculin (51 $\pm$ 7%) compared with cells expressing the single point mutant proteins Y100E and Y1065E (50 $\pm$ 4 and 44 $\pm$ 4%, respectively). In contrast, 65 $\pm$ 3% of the cells expressing the double mutant protein were spread on a fibronectin coated surface by 2 h, representing a 25% increase in the number of spread cells as compared with the other three cell popula-
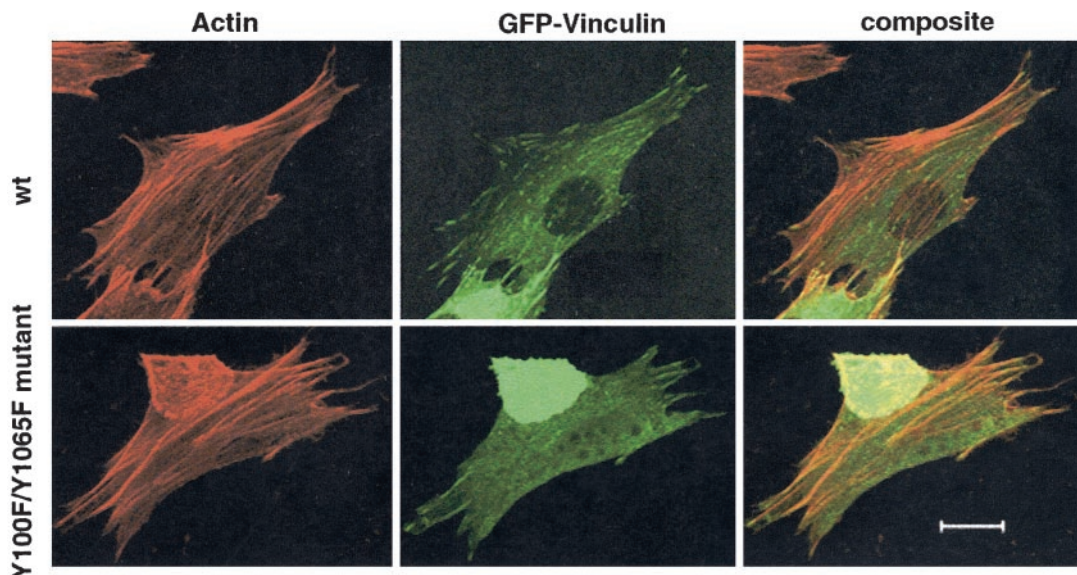

Figure 10. Double phosphorylation mutant protein Y100F/Y1065F is localized to focal adhesion plaques. NIH 3T3 cells were transfected with either a GFP-wild-type vinculin cDNA (wt) or a GFP-Y100F/Y1065F double mutant cDNA. The cells were fixed, permeabilized, and stained with the F-actin binding drug Texas Red-phalloidin. The cells were imaged by confocal microscopy. Bar, 20 μm.
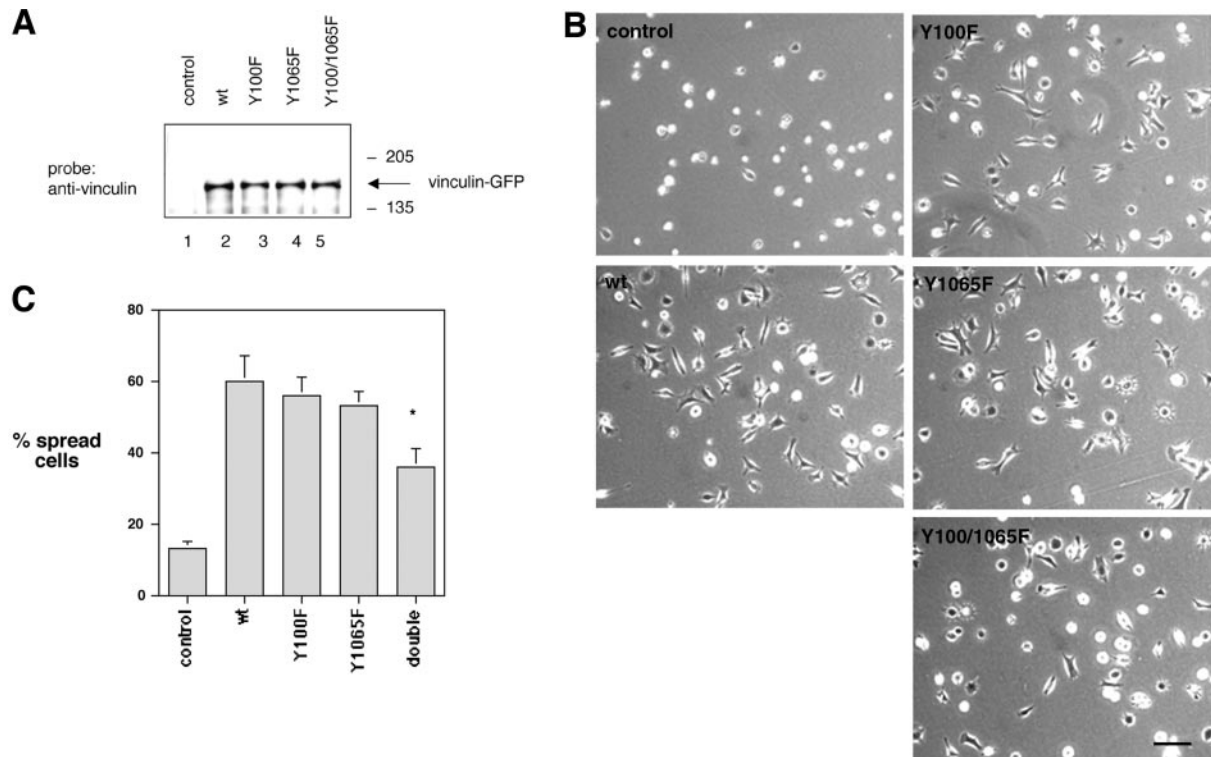
Figure 11. Effect of wild-type and vinculin mutant proteins on cell spreading. Vinculin null cells were transfected with a cDNA encoding a puromycin resistant gene alone (control) or were cotransfected with cDNAs encoding for wild-type vinculin (wt) or the vinculin mutant proteins Y100F, Y1065F, or Y100F/Y1065F. (A) Lysates of puromycin resistant cultures were probed on Western blots with the mAb to vinculin. (B) Puromycin-resistant cells were allowed to spread on fibronectin-coated surfaces (10 μg/ml) for 2 h. The cells were fixed and examined by light microscopy. The images shown are representative of each cell population. Bar, 40 μm. (C) Cells in six random microscopic fields were scored as either spread or round for each population. The number of spread cells was expressed as a percentage relative to the total number of cells per field. Each data point represents the average ± SD of six fields. Approximately 500 cells were examined for each population in each experiment. Results are representative of three experiments. The difference in spreading between cells expressing the double mutant protein Y100F/Y1065F compared with cells expressing wt, Y100F, or Y1065F vinculin proteins was statistically significant (p ≤ 0.001) for all three comparisons.

tions. The difference between the cells expressing the Y100E/Y1065E mutant protein and the cells expressing wild-type vinculin, Y100E or Y1065E mutant proteins was statistically significant (p ≤ 0.001 for all three comparisons).

DISCUSSION

Cell adhesion to the extracellular matrix triggers a rapid and dynamic assembly of multiprotein complexes that is driven by integrins. The protein complexes serve as a platform for coupling integrins to the actin polymerization and assembly machinery. The earliest identified multiprotein complexes, referred to as "focal complexes" contain integrin(s), talin, paxillin, α-actinin, and low levels of vinculin and FAK (Zaidel-Bar *et al.*, 2003). The focal complexes are also rich in tyrosine phosphorylated proteins, indicating that kinases are among the first proteins to be recruited and/or activated at these sites. In platelets, the $\alpha_{IIb}\beta_3$-integrin receptor constitutively interacts with Src kinases; the kinases are activated as a consequence of $\alpha_{IIb}\beta_3$-activation and ligation (Kralisz and Cierniewski, 1998; Obergfell *et al.*, 2002; Arias-Salgado *et al.*, 2003). Platelets pretreated in vitro with an inhibitor of Src kinases, PP2, and murine platelets harvested from Src family kinase-deficient mice, failed to spread on fibrinogen, the primary integrin $\alpha_{IIb}\beta_3$ extracellular matrix ligand (Obergfell *et al.*, 2002). Similarly, triple Src-, Yes-, and

Fyn-kinase–deficient fibroblasts exhibited impaired cell migration and spreading on fibronectin (Klinghoffer *et al.*, 1999; Cary *et al.*, 2002). These findings established that Src kinases are key, early components, in the signal transduction pathway(s) from integrins to the cytoskeleton. The tyrosine kinase Syk and its downstream effector substrates Vav1, Vav3, and SLAP-130 were implicated as one signal transduction pathway linking $\alpha_{IIb}\beta_3$ and Src kinases to the cytoskeleton (Obergfell *et al.*, 2002). Our results indicating that vinculin is tyrosine phosphorylated by Src kinases in platelets, and in reconstituted COS-7 cells, open the door to the possibility that Src kinases also may use vinculin as a vehicle to relay integrin-dependent signals to the actin cytoskeleton.

The data reported in this study demonstrate that endogenous vinculin is phosphorylated on tyrosine residue 1065 in spread platelets. The phosphorylation was not detected in unstimulated platelets or in platelets treated with the inhibitor of Src kinases, PP2. The phosphorylation of vinculin on tyrosine residue 1065 was reconstituted in vanadate-treated cells cotransfected with wild-type vinculin and a constitutively active c-Src kinase. Tyrosine residue 1065 was also phosphorylated by c-Src in vitro, thus establishing that this residue is a bona fide Src kinases substrate. Using the reconstituted COS-7 system, we identified a second phosphorylation site on residue 100. Unlike residue 1065, residue 100 was not phosphorylated by c-Src in vitro, raising the possibility

that the phosphorylation of vinculin may be regulated by two, or more, distinct kinases. Importantly, we also found that although the single point mutant proteins (Y100F and Y1065F) were as effective as wild vinculin in rescuing the spreading defect of vinculin −/− cells on fibronectin, the double mutant protein (Y100F/Y1065F) was significantly less effective than wild-type vinculin, or the single point mutants. Furthermore, a second double mutant protein carrying negative charges in place of the tyrosine residues in position 100 and 1065 (Y100E/Y1065E) was significantly more effective than wild-type vinculin in rescuing the spreading defect of vinculin −/− cells on fibronectin. It is therefore possible that the activity of vinculin is optimal only when both sites are phosphorylated.

Biochemical and crystal structure data demonstrated that vinculin exists in closed and open conformations. Vinculin is held in an inactive, closed conformation by intramolecular interactions between its head and tail domains (Johnson and Craig, 1994; Bakolitsa et al., 1999, 2004; Borgon et al., 2004; Izard et al., 2004). The actin binding site in vinculin is masked when vinculin is in its closed conformation (Johnson and Craig, 1995). Binding of acidic phospholipids to the vinculin tail domain affects head–tail interactions and converts vinculin to an active, ligand-binding competent form (Gilmore and Burridge, 1996; Weekes et al., 1996). Crystal structures recently resolved by Izard et al. (2004) further revealed that binding of talin derived peptides to the vinculin head domain induces a marked conformation change in the vinculin head domain, resulting in tail displacement. Binding of α-actinin to vinculin similarly affected vinculin's head–tail interaction (Izard et al., 2004). These observations established that the conversion of vinculin from a closed to an open conformation is regulated by several, alternative mechanisms. Based on the observation that the phosphorylation of vinculin on tyrosine residue 1065 reduced head–tail interaction in vitro, we speculated that the phosphorylation of vinculin by Src kinases also could positively regulate the activation state of vinculin. In at least one analogous situation, the valosin-containing protein (VCP) was found to be phosphorylated on tyrosine residue 805, the penultimate residue in the protein (Egerton et al., 1992). The phosphorylation of VCP on residue 805 disrupted intramolecular head–tail interactions, which in turn exposed a nuclear-targeting sequence in the VCP head domain (Madeo et al., 1998). Similarly, the phosphorylation of ezrin on a threonine residue caused conformational changes that unmasked both membrane and actin binding sites in the protein (Fievet et al., 2004). Here, we show that phosphorylated vinculin did not cosediment with polymerized actin, suggesting that the actin binding site in vinculin remained masked despite the phosphorylation. It thus seems that the primary function of the phosphorylation of vinculin on serine residues 1033 and 1045 (Ziegler et al., 2002) or tyrosine residues 100 and 1065 is not to modulate the interaction between vinculin and actin. The change(s) in conformation brought about by the phosphorylation might impact the interaction of vinculin with other proteins, and/or determines how long vinculin is in an open conformation. The recent study by Subauste et al. (2004) suggesting that the vinculin tail domain could modulate the interaction between paxillin and FAK highlights one mechanism by which a change in the tail conformation may affect cellular responses.

Vinculin is a well-established constituent of focal adhesion plaques. Recent studies revealed that the localization of some focal adhesion components is regulated by their state of phosphorylation. Interestingly, FAK and α-actinin, two of the proteins thought to directly interact with integrins (Otey

et al., 1990; Schaller et al., 1995), were excluded from focal adhesion plaques when phosphorylated on tyrosine residues (Katz et al., 2003; von Wichert et al., 2003). These observations raised the possibility that the density of proteins such as FAK and α-actinin within the plaque is regulated. We have no evidence at the present time that the localization of vinculin to focal adhesion plaques is similarly affected by its state of phosphorylation; in fact, two lines of evidence argue against this possibility. First, we found that the vinculin double mutant Y100F/Y1065F and Y100E/Y1065E (unpublished data) localized to focal adhesion plaques. In addition, Volberg et al. (2001) reported that vinculin localized to focal adhesion plaques in Src, Yes, and Fyn triple null cells. These findings, however, do not exclude the possibility that the phosphorylation of vinculin by Src kinases affects the dynamics of its recruitment and/or residency time within the early focal complexes, where it may play an important role in regulating the assembly of actin filaments, possibly through an Arp 2/3-dependent mechanism (DeMali et al., 2002).

Ziegler et al. (2002) proposed that the phosphorylation of vinculin by protein kinase C may regulate the incorporation of vinculin into nascent cell adhesion complexes. In fact, it is possible that both Src and protein kinase C enzyme families regulate the dynamics of vinculin assembly into plaques. Indeed, treatment of platelets with PMA, a protein kinase C activator, triggered robust phosphorylation of vinculin, whereas treatment of the platelets with bisindolylmaleimide, an inhibitor of protein kinase C (Toullec et al., 1991), inhibited platelet spreading on fibrinogen as well as the phosphorylation of vinculin on tyrosine 1065 (Zhang, Lin, and Haimovich, unpublished data). It is also possible that as shown in T cells, protein kinase C regulates the activity of a Src kinase family member(s) (Niu et al., 2003). Further studies are required to determine whether platelet vinculin is phosphorylated on serine residues 1033 and 1045 and whether the phosphorylation on these sites is a prerequisite for the phosphorylation on tyrosine residue 1065.

The crystal structure of chicken vinculin tail domain (residues 879-1066), the human vinculin head (residues 1–258), and tail (residues 879-1066) domain complex, and that of intact vinculin were resolved previously (Bakolitsa et al., 1999, 2004; Borgon et al., 2004; Izard et al., 2004). In the intact vinculin, residue 100 is fully exposed, whereas residue 1065 is occluded by a stretch of amino acids derived from the proline-rich region (Bakolitsa et al., 2004). The fact that residue 1065 is buried explains why intact vinculin was not phosphorylated by c-Src in vitro (Zhang, Lin, and Haimovich, unpublished data) and is consistent with the possibility that the phosphorylation of vinculin by c-Src requires a priming input. The atomic structure of the vinculin tail domain revealed a bundle of five helices connected by short loops and packed in an antiparallel orientation with the N- and C-terminal ends emerging from the same side of the bundle (Bakolitsa et al., 1999). Extending from the last helix is a stretch of 21 amino acids, referred to as the C-terminal arm (1045–1066). Bakoltisa et al. (1999) identified three potential regions within the C-terminal arm: a flexible loop (1047–1052), a β clamp (1053–1061), and a hydrophobic hairpin (1062–1066). A mutant protein lacking residues 1052–1066 failed to cosediment with acidic phospholipid vesicles at a physiological pH (Bakolitsa et al., 1999). This observation, the hydrophobic nature of the vinculin hairpin tail, and the possibility that tryptophans may orient proteins toward membranes, or perhaps play a role in the bilayer

insertion process (Wallace and Janes, 1999), led Bakolitsa *et al.* (1999) to propose that the last five amino acid residues in vinculin, Thr-ProTrp-Tyr-Gln (TPWYQ), are inserted into membranes. Whether this observation holds true or not for the intact protein is a question that needs to be addressed in more detail because Johnson *et al.* (1998) have shown that native vinculin does not spontaneously associate with acidic phospholipid vesicles under physiological conditions. The phosphorylation of vinculin on residue 1065 may generate a transient conformation that is more favorable for membrane recognition than the unphosphorylated tail, particularly if, as our data suggest, this phosphorylation affects head–tail interactions. One intriguing possibility is that the phosphorylation may help unmask residues 916–970 shown to interact with, and insert into, acidic phospholipids (Johnson *et al.*, 1998). On the other hand, it is also possible that the phosphorylation creates a deliberate obstacle for the membrane insertion step and thus serves to regulate the membrane binding activity of vinculin, and/or the targeting of vinculin to specific sites, where it may help facilitate the assembly of actin filaments. As a follow-up to this notion, it is also possible to envision that the recruitment of vinculin to specific sites is regulated by a phosphatase that can rapidly dephosphorylate vinculin thus rendering the phosphorylation a transient event. This may explain why the phosphorylation of vinculin in COS-7 cells is not detected unless the cells are pretreated with vanadate. Such a model would also imply that the activation state of vinculin is tightly regulated by Src kinases and a counteracting phosphatase(s).

α-Actinin (Izaguirre *et al.*, 1999) and as shown here, vinculin, undergo robust tyrosine phosphorylation in spread platelets. The significance of these tyrosine phosphorylation events is clearly not limited to platelets (von Wichert *et al.*, 2003) but rather is easier to detect in platelets than in other types. Why is that the case? It seems that platelet spreading is an "all-out" process. Because platelet spreading is an irreversible process, platelets can afford to unleash robust tyrosine phosphorylation of proteins that are only transiently or sparsely phosphorylated in other cell types thus limiting their detection. Considering the large number of proteins that are phosphorylated on tyrosine in spread platelets this system should prove to be informative in efforts to dissect events regulating focal adhesion assembly.

ACKNOWLEDGMENTS

REFERENCES

Arias-Salgado, E.G., Lizano, S., Sarkar, S., Brugge, J.S., Ginsberg, M.H., and Shattil, S.J. (2003). Src kinase activation by direct interaction with the integrin beta cytoplasmic domain. Proc. Natl. Acad. Sci. USA *100*, 13298–13302.

Bakolitsa, C., Cohen, D.M., Bankston, L.A., Bobkov, A.A., Cadwell, G.W., Jennings, L., Critchley, D.R., Craig, S.W., and Liddington, R.C. (2004). Structural basis for vinculin activation at sites of cell adhesion. Nature *13*, 22.

Bakolitsa, C., de Pereda, J.M., Bagshaw, C.R., Critchley, D.R., and Liddington, R.C. (1999). Crystal structure of the vinculin tail suggests a pathway for activation. Cell *99*, 603–613.

Borgon, R.A., Vonrhein, C., Bricogne, G., Bois, P.R.J., and Izard, T. (2004). Crystal structure of human vinculin. Structure *12*, 1189–1197.

Bruin, T., Asijee, G.M., Prins, A., ten Cate, J.W., and Sturk, A. (1991). Subcellular distribution and phosphorylation of vinculin isoforms in human blood platelets. Thromb. Haemost. *65*, 206–211.

Cary, L.A., Klinghoffer, R.A., Sachsenmaier, C., and Cooper, J.A. (2002). SRC catalytic but not scaffolding function is needed for integrin-regulated tyrosine phosphorylation, cell migration, and cell spreading. Mol. Cell. Biol. *22*, 2427–2440.

Coutu, M.D., and Craig, S.W. (1988). cDNA-derived sequence of chicken embryo vinculin. Proc. Natl. Acad. Sci. USA *85*, 8535–8539.

Critchley, D.R. (2000). Focal adhesions - the cytoskeletal connection. Curr. Opin. Cell Biol. *12*, 133–139.

DeMali, K.A., Barlow, C.A., and Burridge, K. (2002). Recruitment of the Arp2/3 complex to vinculin: coupling membrane protrusion to matrix adhesion. J. Cell Biol. *159*, 881–891.

Egerton, M., Ashe, O.R., Chen, D., Druker, B.J., Burgess, W.H., and Samelson, L.E. (1992). VCP, the mammalian homolog of cdc48, is tyrosine phosphorylated in response to T cell antigen receptor activation. EMBO J. *11*, 3533–3540.

Emsley, J., Knight, C.G., Farndale, R.W., Barnes, M.J., and Liddington, R.C. (2000). Structural basis of collagen recognition by integrin alpha2beta1. Cell *101*, 47–56.

Fievet, B.T., Gautreau, A., Roy, C., Del Maestro, L., Mangeat, P., Louvard, D., and Arpin, M. (2004). Phosphoinositide binding and phosphorylation act sequentially in the activation mechanism of ezrin. J. Cell Biol. *164*, 653–659.

Geiger, B., Bershadsky, A., Pankov, R., and Yamada, K.M. (2001). Transmembrane crosstalk between the extracellular matrix–cytoskeleton crosstalk. Nat. Rev. Mol. Cell. Biol. *2*, 793–805.

Geiger, B., Tokuyasu, K.T., Dutton, A.H., and Singer, S.J. (1980). Vinculin, an intracellular protein localized at specialized sites where microfilament bundles terminate at cell membranes. Proc. Natl. Acad. Sci. USA *77*, 4127–4131.

Gilmore, A.P., and Burridge, K. (1996). Regulation of vinculin binding to talin and actin by phosphatidyl-inositol-4–5-bisphosphate. Nature *381*, 531–535.

Golden, A., Nemeth, S.P., and Brugge, J.S. (1986). Blood platelets express high levels of the pp60c-src-specific tyrosine kinase activity. Proc. Natl. Acad. Sci. USA *83*, 852–856.

Goldmann, W.H., Guttenberg, Z., Tang, J.X., Kroy, K., Isenberg, G., and Ezzell, R.M. (1998). Analysis of the F-actin binding fragments of vinculin using stopped-flow and dynamic light-scattering measurements. Eur. J. Biochem. *254*, 413–419.

Goldmann, W.H., and Ingber, D.E. (2002). Intact vinculin protein is required for control of cell shape, cell mechanics, and rac-dependent lamellipodia formation. Biochem. Biophys. Res. Commun. *290*, 749–755.

Gravel, P., Sanchez, J.-C., Walzer, C., Golaz, O., Hochstrasser, D.F., Balant, L.P., Hughes, G.J., Garcia-Sevilla, J., and Guimon, J. (1995). Human blood platelet protein map established by two-dimensional polyacrylamide gel electrophoresis. Electrophoresis *16*, 1152–1159.

Gu, J., Tamura, M., Pankov, R., Danen, E.H., Takino, T., Matsumoto, K., and Yamada, K.M. (1999). Shc and FAK differentially regulate cell motility and directionality modulated by PTEN. J. Cell Biol. *146*, 389–403.

Haimovich, B., Lipfert, L., Brugge, J.S., and Shattil, S.J. (1993). Tyrosine phosphorylation and cytoskeletal reorganization in platelets are triggered by interaction of integrin receptors with their immobilized ligands. J. Biol. Chem. *268*, 15868–15877.

Hanke, J.H., Gardner, J.P., Dow, R.L., Changelian, P.S., Brissette, W.H., Weringer, E.J., Pollok, B.A., and Connelly, P.A. (1996). Discovery of a novel, potent, and Src family-selective tyrosine kinase inhibitor. Study of Lck- and FynT-dependent T cell activation. J. Biol. Chem. *271*, 695–701.

Huang, M.M., Bolen, J.B., Barnwell, J.W., Shattil, S.J., and Brugge, J.S. (1991). Membrane glycoprotein IV (CD36) is physically associated with the Fyn, Lyn, and Yes protein-tyrosine kinases in human platelets. Proc. Natl. Acad. Sci. USA *88*, 7844–7848.

Huttelmaier, S., Bubeck, P., Rudiger, M., and Jockusch, B.M. (1997). Characterization of two F-actin-binding and oligomerization sites in the cell-contact protein vinculin. Eur. J. Biochem. *247*, 1136–1142.

Huttelmaier, S., Mayboroda, O., Harbeck, B., Jarchau, T., Jockusch, B.M., and Rudiger, M. (1998). The interaction of the cell-contact proteins VASP and vinculin is regulated by phosphatidylinositol-4,5-bisphosphate. Curr. Biol. *8*, 479–488.

Hynes, R.O. (2002). Integrins: bidirectional, allosteric signaling machines. Cell *110*, 673–687.

Ito, S., Werth, D.K., Richert, N.D., and Pastan, I. (1983). Vinculin phosphorylation by the src kinase. Interaction of vinculin with phospholipid vesicles. J. Biol. Chem. *258*, 14626–14631.

Izaguirre, G., Aguirre, L., Hu, Y.P., Lee, H.Y., Schlaepfer, D.D., Aneskievich, B.J., and Haimovich, B. (2001). The cytoskeletal/non-muscle isoform of alpha-actinin is phosphorylated on its actin-binding domain by the focal adhesion kinase. J. Biol. Chem. *276*, 28676–28685.

Izaguirre, G., Aguirre, L., Ji, P., Aneskievich, B., and Haimovich, B. (1999). Tyrosine phosphorylation of alpha-actinin in activated platelets. J. Biol. Chem. *274*, 37012–37020.

Izard, T., Evans, G., Borgon, R.A., Rush, C.L., Bricogne, G., and Bois, P.R. (2004). Vinculin activation by talin through helical bundle conversion. Nature *427*, 171–175.

Johnson, R.P., and Craig, S.W. (1994). An intramolecular association between the head and tail domains of vinculin modulates talin binding. J. Biol. Chem. *269*, 12611–12619.

Johnson, R.P., and Craig, S.W. (1995). F-actin binding site masked by the intramolecular association of vinculin head and tail domains. Nature *373*, 261–264.

Johnson, R.P., and Craig, S.W. (2000). Actin activates a cryptic dimerization potential of the vinculin tail domain. J. Biol. Chem. *275*, 95–105.

Johnson, R.P., Niggli, V., Durrer, P., and Craig, S.W. (1998). A conserved motif in the tail domain of vinculin mediates association with and insertion into acidic phospholipid bilayers. Biochemistry *37*, 10211–10222.

Katz, B.Z., Romer, L., Miyamoto, S., Volberg, T., Matsumoto, K., Cukierman, E., Geiger, B., and Yamada, K.M. (2003). Targeting membrane-localized focal adhesion kinase to focal adhesions: roles of tyrosine phosphorylation and SRC family kinases. J. Biol. Chem. *278*, 29115–29120.

Kawabe, H., Hata, Y., Takeuchi, M., Ide, N., Mizoguchi, A., and Takai, Y. (1999). nArgBP2, a novel neural member of ponsin/ArgBP2/vinexin family that interacts with synapse-associated protein 90/postsynaptic density-95-associated protein (SAPAP). J. Biol. Chem. *274*, 30914–30918.

Kim, M., Carman, C.V., and Springer, T.A. (2003). Bidirectional transmembrane signaling by cytoplasmic domain separation in integrins. Science *301*, 1720–1725.

Klinghoffer, R.A., Sachsenmaier, C., Cooper, J.A., and Soriano, P. (1999). Src family kinases are required for integrin but not PDGFR signal transduction. EMBO J. *18*, 2459–2471.

Kralisz, U., and Cierniewski, C.S. (1998). Association of pp60c-src with alpha IIb beta 3 in resting platelets. Biochem. Mol. Biol. Int. *45*, 735–743.

Liu, S., Calderwood, D.A., and Ginsberg, M.H. (2000). Integrin cytoplasmic domain-binding proteins. J. Cell Sci. *113*, 3563–3571.

Madeo, F., Schlauer, J., Zischka, H., Mecke, D., and Frohlich, K.U. (1998). Tyrosine phosphorylation regulates cell cycle-dependent nuclear localization of Cdc48p. Mol. Biol. Cell *9*, 131–141.

Mandai, K., Nakanishi, H., Satoh, A., Takahashi, K., Satoh, K., Nishioka, H., Mizoguchi, A., and Takai, Y. (1999). Ponsin/SH3P *12*, an l-afadin- and vinculin-binding protein localized at cell-cell and cell-matrix adherens junctions. J. Cell Biol. *144*, 1001–1017.

Massoumi, R., and Sjolander, A. (2001). Leukotriene D(4) affects localisation of vinculin in intestinal epithelial cells via distinct tyrosine kinase and protein kinase C controlled events. J. Cell Sci. *114*, 1925–1934.

Menkel, A.R., Kroemker, M., Bubeck, P., Ronsiek, M., Nikolai, G., and Jockusch, B.M. (1994). Characterization of an F-actin-binding domain in the cytoskeletal protein vinculin. J. Cell Biol. *126*, 1231–1240.

Niu, S., Xie, H., and Marcantonio, E.E. (2003). Integrin-mediated tyrosine phosphorylation of Shc in T cells is regulated by protein kinase C-dependent phosphorylations of Lck. Mol. Biol. Cell *14*, 349–360.

Obergfell, A., Eto, K., Mocsai, A., Buenseceso, C., Moores, S.L., Brugge, J.S., Lowell, C.A., and Shattil, S.J. (2002). Coordinate interactions of Csk, Src, and Syk kinases with [alpha]IIb[beta]3 initiate integrin signaling to the cytoskeleton. J. Cell Biol. *157*, 265–275.

Otey, C.A., Pavalko, F.M., and Burridge, K. (1990). An interaction between α-actinin and the β1 integrin subunit *in vitro*. J. Cell Biol. *11*, 721–729.

Pinna, L.A., and Ruzzene, M. (1996). How do protein kinases recognize their substrates? Biochim. Biophys. Acta *1314*, 191–225.

Ridley, A.J., Schwartz, M.A., Burridge, K., Firtel, R.A., Ginsberg, M.H., Borisy, G., Parsons, J.T., and Horwitz, A.R. (2003). Cell migration: integrating signals from front to back. Science *302*, 1704–1709.

Schaller, M.D., Otey, C.A., Hildebrand, J.D., and Parsons, J.T. (1995). Focal adhesion kinase and paxillin bind to peptides mimicking β integrin cytoplasmic domains. J. Cell Biol. *130*, 1181–1187.

Sefton, B.M., Hunter, T., Ball, E.H., and Singer, S.J. (1981). Vinculin: a cytoskeletal target of the transforming protein of Rous sarcoma virus. Cell *24*, 165–174.

Steimle, P.A., Hoffert, J.D., Adey, N.B., and Craig, S.W. (1999). Polyphosphoinositides inhibit the interaction of vinculin with actin filaments. J. Biol. Chem. *274*, 18414–18420.

Subauste, M.C., Pertz, O., Adamson, E.D., Turner, C.E., Junger, S., and Hahn, K.M. (2004). Vinculin modulation of paxillin-FAK interactions regulates ERK to control survival and motility. J. Cell Biol. *165*, 371–381.

Toullec, D., *et al*. (1991). The bisindolylmaleimide GF 109203X is a potent and selective inhibitor of protein kinase C. J. Biol. Chem. *266*, 15771–15781.

Volberg, T., Romer, L., Zamir, E., and Geiger, B. (2001). pp60(c-src) and related tyrosine kinases: a role in the assembly and reorganization of matrix adhesions. J. Cell Sci. *114*, 2279–2289.

von Wichert, G., Haimovich, B., Feng, G.S., and Sheetz, M.P. (2003). Force-dependent integrin-cytoskeleton linkage formation requires downregulation of focal complex dynamics by Shp2. EMBO J. *22*, 5023–5035.

Vostal, J.G., and Shulman, N.R. (1993). Vinculin is a major platelet protein that undergoes Ca(2+)-dependent tyrosine phosphorylation. Biochem. J. *294*, 675–680.

Wallace, B.A., and Janes, R.W. (1999). Tryptophans in membrane proteins. X-ray crystallographic analyses. Adv. Exp. Med. Biol. *467*, 789–799.

Weekes, J., Barry, S.T., and Critchley, D.R. (1996). Acidic phospholipids inhibit the intramolecular association between the N- and C-terminal regions of vinculin, exposing actin-binding and protein kinase C phosphorylation sites. Biochem. J. *314*, 827–832.

Winkler, J., Lunsdorf, H., and Jockusch, B.M. (1996). The ultrastructure of chicken gizzard vinculin as visualized by high-resolution electron microscopy. J. Struct. Biol. *116*, 270–277.

Wood, C.K., Turner, C.E., Jackson, P., and Critchley, D.R. (1994). Characterisation of the paxillin-binding site and the C-terminal focal adhesion targeting sequence in vinculin. J. Cell Sci. *107*, 709–717.

Xu, W., Baribault, H., and Adamson, E.D. (1998a). Vinculin knockout results in heart and brain defects during embryonic development. Development *125*, 327–337.

Xu, W., Coll, J.L., and Adamson, E.D. (1998b). Rescue of the mutant phenotype by reexpression of full-length vinculin in null F9 cells; effects on cell locomotion by domain deleted vinculin. J. Cell Sci. *111*, 1535–1544.

Zaidel-Bar, R., Ballestrem, C., Kam, Z., and Geiger, B. (2003). Early molecular events in the assembly of matrix adhesions at the leading edge of migrating cells. J. Cell Sci. *116*, 4605–4613.

Ziegler, W.H., Tigges, U., Zieseniss, A., and Jockusch, B.M. (2002). A lipid-regulated docking site on vinculin for protein kinase C. J. Biol. Chem. *277*, 7396–7404.